Context-dependent effect of sPLA$_2$-IIA induced proliferation on murine hair follicle stem cells and human epithelial cancer

Gopal L. Chovatiya [a,b,1], Raghava R. Sunkara [a,b,1], Sayoni Roy [a,b,2], Saloni R. Godbole [a,2], Sanjeev K. Waghmare [a,b,*]

[a] Stem Cell Biology Group, Waghmare Lab, Cancer Research Institute, Advanced Centre for Treatment Research and Education in Cancer (ACTREC), Tata Memorial Centre, Kharghar, Navi Mumbai 410210, Maharashtra, India
[b] Homi Bhabha National Institute, Training School Complex, Anushakti Nagar, Mumbai 400085, India

ABSTRACT

Background: Tissue stem cells (SCs) and cancer cells proliferation is regulated by many common signalling mechanisms. These mechanisms temporally balance proliferation and differentiation events during normal tissue homeostasis and repair. However, the effect of these aberrant signalling mechanisms on the ultimate fate of SCs and cancer cells remains obscure.

Methods: To evaluate the functional effects of Secretory Phospholipase A$_2$-IIA (sPLA$_2$-IIA) induced abnormal signalling on normal SCs and cancer cells, we have used K14-sPLA$_2$-IIA transgenic mice hair follicle stem cells (HFSCs), DMBA/TPA induced mouse skin tumour tissues, human oral squamous cell carcinoma (OSCC) and skin squamous cell carcinoma (SCC) derived cell lines.

Findings: Our study demonstrates that sPLA$_2$-IIA induces rapid proliferation of HFSCs, thereby altering the proliferation dynamics leading to a complete loss of the slow cycling H2BGFP positive HFSCs. Interestingly, *in vivo* reversion study by JNK inhibition exhibited a significant delay in post depilation hair growth, confirming that sPLA$_2$-IIA promotes HFSCs proliferation through JNK/c-Jun signalling. In a different cellular context, we showed increased expression of sPLA$_2$-IIA in human OSCC and mouse skin cancer tissues. Importantly, a xenograft of sPLA$_2$-IIA knockdown cells of OSCC and SCC cell lines showed a concomitant reduction of tumour volume in NOD-SCID mice and decreased JNK/c-Jun signalling.

Interpretation: This study unravels how an increased proliferation induced by a common proliferation inducer (sPLA$_2$-IIA) alters the fate of normal SCs and cancer cells distinctively through common JNK/c-Jun signalling. Thus, sPLA$_2$-IIA can be a potential target for various diseases including cancer.

Fund: This work was partly supported by the Indian Council of Medical Research (ICMR-3097) and ACTREC (42) grants.

1. Introduction

Adult stem cells (SCs) possess long-term regenerative potential and maintain tissue integrity during homeostasis. These long-lived SCs, within the niche, protect their genomic integrity through rare cell divisions. The advent of DNA labelling techniques has provided enormous information about the location and cyclic behaviour of the slow-cycling SCs in various tissues. Importantly, a novel double transgenic mouse, expressing H2BGFP (Tet-Off) under the control of a tissue-specific promoter, has greatly enhanced our understanding on slow cycling characteristic of adult SCs. In particular, HFSCs within the bulge of the hair follicle are highly dynamic and display asynchronous division characteristics. The H2BGFP positive label-retaining cells (LRCs) from the hair follicle were isolated by using pTRE-H2BGFP:K5tTA double transgenic mice, which paved the way to unravel factors responsible for maintenance of the stemness characteristic and SCs niche [1]. Further, infrequent proliferation dynamics of HFSCs was shown by Waghmare et al., 2008, which provided the first evidence of differential quiescence potential and information about the differential rate of the HFSCs division within the bulge [2,3]. In addition, the H2BGFP system was also exploited to identify a heterogeneous population of the hematopoietic SCs and the intestinal SCs [4–6]. However, the cross-talk of various signalling mechanisms that maintain the differential quiescence potential and HFSCs division rate within the bulge is poorly understood.

Secreted phospholipases A$_2$ (sPLA$_2$s) catalyze the conversion of glycerophospholipids to release free fatty acids and lysophospholipids [7]. sPLA$_2$ family isoforms of human and mice share high structural

Research in context

Evidence before this study

sPLA$_2$-IIA is involved in different patho-physiological processes such as arthritis, inflammation and cancer. Also, deregulated expression of secretory phospholipase family proteins, mainly sPLA$_2$-IIA, has been reported in diverse human cancers. However, the mechanism through which sPLA$_2$-IIA modulates the downstream signalling cascades, and the effect of this altered signalling on the proliferation dynamics of the adult SCs and epithelial cancer cells remain poorly understood.

Added value of this study

This study unraveled the differential effect of sPLA$_2$-IIA on normal SC pool maintenance and cancer cell proliferation. sPLA$_2$-IIA induced rapid HFSC proliferation through c-Jun signalling, which resulted in a loss of infrequent divisions and stemness characteristics, and eventually led to the exhaustion of tissue SC pool. In contrast, sPLA$_2$-IIA showed a proliferative advantage to the OSCC cells and promotes rapid tumour growth *in vivo*. This study provides an example of how a common proliferation inducer exhibits differential effect under different cellular contexts.

Implications of all the available evidence

Our study for the first time showed that increased expression of sPLA$_2$-IIA affects the proliferation dynamics of tissue SCs. This study will be useful in designing similar approaches to understand the proliferation dynamics of the tissue SCs during normal or diseased conditions, caused by intrinsic or extrinsic insults. In a different cellular context, upregulated sPLA$_2$-IIA expression in OSCC cell lines derived from Indian patients showed increased proliferation with higher tumorigenic potential. However, knockdown of sPLA$_2$-IIA in OSCC and SCC cell lines showed decreased *in vivo* tumorigenicity. In addition, sPLA$_2$-IIA expression analysis in OSCC tissues also revealed increased expression of sPLA$_2$-IIA. Overall, our study suggests the importance of sPLA$_2$-IIA in future therapeutic implications.

and functional similarity [8], and most sPLA$_2$ isoforms require high calcium concentration for optimal catalytic activity [9]. Secretory phospholipases are known to be involved in a wide range of physiological and pathophysiological conditions [10]. In fact, sPLA$_2$-IIA modulate tumorigenesis of the prostate [11], colon [12], gastric adenocarcinoma [13], lung [14] and oesophageal cancers [15]. Besides, sPLA$_2$ also induces proliferation of astrocytoma and microglia cells [16,17], suggesting its ability to promote cellular proliferation in a wide range of normal and transformed tissue types. In the skin, sPLA$_2$-IIA is predominantly expressed in the proliferating keratinocytes of the basal layer of the epidermis [18,19]. Moreover, overexpression of sPLA$_2$-IIA in transgenic mice led to epidermal hyperplasia and alopecia [20–22]. However, how the sPLA$_2$-IIA affects the long-term maintenance of HFSC pool and its ultimate fate in the *in vivo* system is yet to be investigated. Similarly, overexpression of group III sPLA$_2$ (*PLA2G3*) exhibited skin inflammation and sebaceous gland hyperplasia [23]. Also, transgenic mice overexpressing sPLA$_2$-X (*PLA2G10-Tg*) developed alopecia and showed hair follicle abnormalities with sebaceous glands hyperplasia [24]. A recent study on *Pla2g2f* knockout mice showed the development of fragile stratum corneum and these mice were protected from psoriasis, contact dermatitis and skin cancer development. Conversely, overexpression of *Pla2g2f* in transgenic mice displayed epidermal hyperplasia and altered keratinocytes differentiation [25].

Notably, different epithelial tissues such as skin and oral epithelium exhibit a similar pattern of keratinocyte differentiation, which is a sequential multistep process that is tightly regulated by a variety of signalling modulators. In addition, skin and oral epithelium also share many structural and functional similarities in terms of tissue architecture and response to stress stimuli [26–28]. Therefore, information gained from the study on skin tissue can be extrapolated to other tissues such as oral epithelium to understand the mode of action of the same molecule in similar tissue types. For instance, activator protein 1 (AP1), a transcription factor, is a critical downstream target of MAPK signalling, which regulates keratinocytes proliferation and differentiation [29]. Further, altered AP1 signalling showed aberrant cell proliferation in different pathological conditions such as psoriasis [30] and head and neck squamous cell carcinoma (HNSCC) [31,32]. Importantly, around 50% of the HNSCC tumours display deregulated EGFR signalling, which significantly correlates with poor outcome [33,34]. Also, previous studies have identified a differential role of JNK signalling either as an oncosuppressor or an oncogenic modulator in oral cancer development [35]. Further, sPLA$_2$-IIA is known to induce cell proliferation, however, its effect on the activation of AP1 complex proteins and the subsequent fate of normal and transformed keratinocytes is yet to be discovered.

In the present work, we have studied the context-dependent effect of sPLA$_2$-IIA overexpression in the normal murine HFSCs, human OSCC and SCC cells. We have identified that the sPLA$_2$-IIA induced proliferation alters HFSCs proliferation dynamics and resulted in the survival of a few but rapidly proliferating HFSCs. Further, our data depicted that depilation induces faster hair growth in the K14-sPLA$_2$-IIA mice skin. On the contrary, *in vivo* depilation followed by topical application of the JNK inhibitor (JNK-I) reverted faster hair growth in the K14-sPLA$_2$-IIA mice. In addition, we found upregulation of sPLA$_2$-IIA in OSCC tumour tissues as compared to normal adjacent margin tissues. Further, inhibition of sPLA$_2$-IIA in the OSCC and SCC derived cell lines showed decreased *in vivo* tumorigenic potential of these cancer cells.

2. Materials and methods

2.1. Transgenic mice

K14-sPLA$_2$-IIA transgenic mice were a generous gift from Dr. Rita Mulherkar [36]. pTRE-H2BGFP mice were purchased from Jackson laboratories, USA and K5tTA mice were a kind gift from Dr. Rune Toftgard, Sweden. For proliferation dynamics, we crossed K14-sPLA$_2$-IIA (FVB) and pTRE–H2BGFP (CD1) to obtain hemizygous K14-sPLA$_2$-IIA:pTRE–H2BGFP mice. Further, K14-sPLA$_2$-IIA:pTRE–H2BGFP mice were crossed with K5tTA (FVB1) mice to obtain K14-sPLA$_2$-IIA:pTRE–H2BGFP:K5tTA triple transgenic mice. However, we observed that newborn pups with a combination of H2BGFP and sPLA$_2$-IIA was lethal since the mice died within five days after the birth. However, the H2BGFP positive pups without K14-sPLA$_2$-IIA survived without any mortality. To circumvent the neonatal lethality, female mice having new-born pups were fed with the 0.25 mg/ml Doxycyclin in water for 24 to 48 h, which was sufficient to reduce the level of H2BGFP expression. However, by postnatal day (PD) 21, saturated levels of H2BGFP expression were successfully achieved. All the mice work was approved by ACTREC's Institutional Animal Ethics Committee (IAEC).

2.2. Mouse epidermal keratinocytes culture

Primary mouse epidermal keratinocytes were isolated from the back skin of wild-type and K14-sPLA$_2$-IIA transgenic mice at PD2. Dorsal skin was excised, fat was scraped off from the skin and incubated overnight in Dispase (5 U/ml). Epidermis was separated from the underlying dermis and minced in 0.1% Trypsin-EDTA. Cell suspensions were neutralized by *E*-media that were passed through 70-µm cell strainer. Keratinocytes were cultured in low Ca^{+2} (0.05 mM) containing *E*-media on irradiated mouse J2-3 T3 fibroblasts till seven passages

[37]. For the JNK inhibition study, cells were washed with PBS and treated with different concentrations (0.1, 0.25, 0.5 μM) of JNK inhibitor (JNK-I) (SP600125, Calbiochem) for three days. Proteins were extracted in radioimmunoprecipitation (RIPA) assay buffer for further western blotting analysis as described previously [21].

2.3. Analysis of depilation-induced hair growth

The dorsal skin of wild-type and K14-sPLA$_2$-IIA mice was shaved at PD45 and cleaned with cotton swabs. To synchronize the hair cycle by depilation, hot wax was applied on the dorsal skin and the hair were plucked off by using hair removal strips at PD46. For JNK inhibition study, JNK-I was applied two days before depilation and continued for ten days after depilation. The depilation-induced hair growth was recorded by capturing photographs.

2.4. Immunohistochemistry (IHC) and immunofluorescence assay

Mice were sacrificed at various postnatal days for the hair follicle cycling study, and to determine the effect of 12-O-tetradecanoylphorbol 13-acetate (TPA) or JNK-I treatment. Skin tissues were immediately fixed in 10% neutral buffered formalin (NBF) and further processed for the preparation of paraffin blocks. For cryosectioning, the skin samples were directly embedded in OCT compound (Tissue-Tek). The embedded skin was cryosectioned at 5 to 10-μm thickness on lysine coated slides and used for immunofluorescence staining as described earlier [2,21,22,37,38]. For the IHC of the tumour tissues, the antigen retrieval was performed by heating the slides in 10 mM sodium citrate (pH 6.0) in a microwave for 10 min. Antibodies used for IHC were anti-p-c-Jun (1:100, Abcam), anti-Human sPLA$_2$-IIA (1:50, Abbexa), anti-BrdU (1:100, Abcam) and anti-Ki67 (1:100, Abcam).

2.5. Cell lines and tumour tissue samples

We have used ACOSC3, ACOSC4 and ACOSC16 OSCC cell lines, which were recently established in our laboratory from the advanced stage treatment naïve buccal mucosa tumours [39]. For skin cancer, we have used the human squamous cell carcinoma (SCC) line A3886 obtained from Dr. Colin Jamora's Lab at Instem, Bengaluru [40]. These cell lines were cultured in Minimum Essential Medium (MEM) containing 10% fetal bovine serum and 1% antibiotics (Invitrogen), and maintained at 37 °C with 5% CO$_2$. The tumour tissue samples used in the study were approved by the Institutional Ethics Committee (IEC).

2.6. Western blotting

Skin was collected from the Acetone and TPA treated wild-type and K14-sPLA$_2$-IIA mice and flash-frozen in liquid Nitrogen. The epidermis
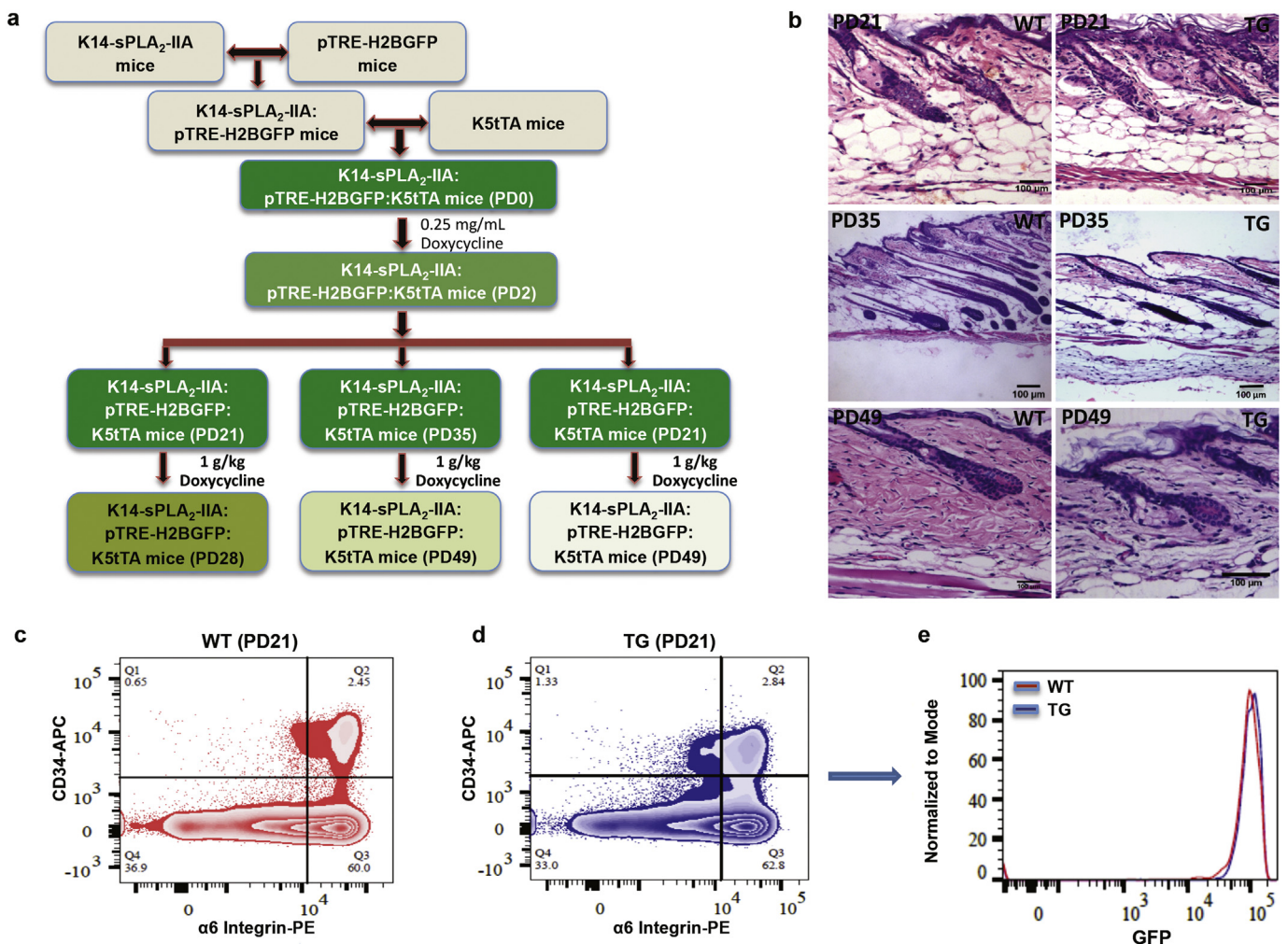
Fig. 1. Development of GFP chasing system and GFP labeling efficiency in K14-sPLA$_2$-IIA mice. a) Scheme of triple transgenic mice generation and doxycycline chasing. b) Hematoxylin and eosin (H&E) staining of dorsal skin sections at PD21, PD35 and PD49. c-d) Scheme for the separation of the HFSCs population from the WT and TG mice skin by using CD34 and α6 integrin markers. e) Intensity of GFP signal in the HFSCs of WT and TG mice at PD21. (WT- Wild type for sPLA$_2$-IIA and positive for H2BGFP:K5tTa, TG- K14-sPLA$_2$-IIA:H2BGFP:K5tTa positive mice, $n = 3$ mice/genotype, Scale bar 100 μm).

was scraped and minced in the RIPA buffer containing protease and phosphatase inhibitors cocktail (Roche). The tissue was homogenized for 10 min and frozen at −80 °C until further use. For the preparation of the whole cell lysates of cultured cells, the cells were washed with ice-cold PBS and scraped in the RIPA buffer. Next, the cell lysate was centrifuged at 16,000 ×g for 30 min at 4 °C. Protein concentration was quantified using Bradford reagent (Sigma) as per manufacturer's instruction. Total 40–60 μg of protein was loaded on 10% SDS-polyacrylamide gel and transferred on to nitrocellulose membrane. Membrane was then blocked with blocking buffer (5% nonfat dry milk or 5% BSA, 10 mM Tris, 150 mM NaCl, 0.1% Tween-20) and probed with the following primary antibodies: p-c-Jun (1:1000), c-Jun (1:1000), p-c-Fos (1:1000), c-Fos (1:1000) all from Cell Signalling Technologies, USA, anti-sPLA$_2$-IIA (1:500) from Merck-Millipore and β-actin (1:10000) from Sigma Aldrich.

2.7. Orosphere formation assay

Three OSCC cell lines (ACOSC3, ACOSC4 and ACOSC16) were used to check their sphere-forming potential in the presence of sPLA$_2$-IIA inhibitor. A single cell suspension of all the three cell lines was made by trypsinization and the number of cells were counted by using hemocytometer. We seeded 40 K cells with 0 μM, 10 μM and 20 μM of sPLA$_2$-IIA inhibitor (LY311727, Sigma Aldrich) in 2 ml of complete MammoCult™ medium per well into ultra-low adherent six-well plates. The plates were incubated at 37 °C with 5% CO$_2$ for 5 days. Total numbers of spheres in each well were counted by using a light microscope. Total number of spheres formed per well in the presence of a different concentration of sPLA$_2$-IIA inhibitor were plotted using GraphPad Prism.

2.8. Knockdown of sPLA$_2$-IIA in tumour cell lines

sPLA$_2$-IIA knockdown in the ACOSC4, ACOSC16 (OSCC) and A3886 (SCC) cell lines was performed using the viral transduction particles obtained from Sigma Aldrich, USA. We have obtained Institutional Biosafety Committee (IBSC) approval to carry out lentiviral transfection. We used the following two different *PLA2G2A* short hairpin RNA sequences described previously [16].

For clone 45- GGGATCAAGTTGACGACAGGAAA
For clone 46- GGTGCTAGAAACAAGACGACCTA

The transfected cells were selected by using 1.5 μg/ml puromycin for 5 days and further expanded for the *in vitro* and *in vivo* studies.

2.9. In vivo tumorigenesis assay

To determine the role of sPLA$_2$-IIA in the *in vivo* tumorigenesis, we subcutaneously injected 1×10^6 *PLA2G2A* knockdown/vector control cells in 100 μl MEM medium with Matrigel into NOD-SCID xenograft
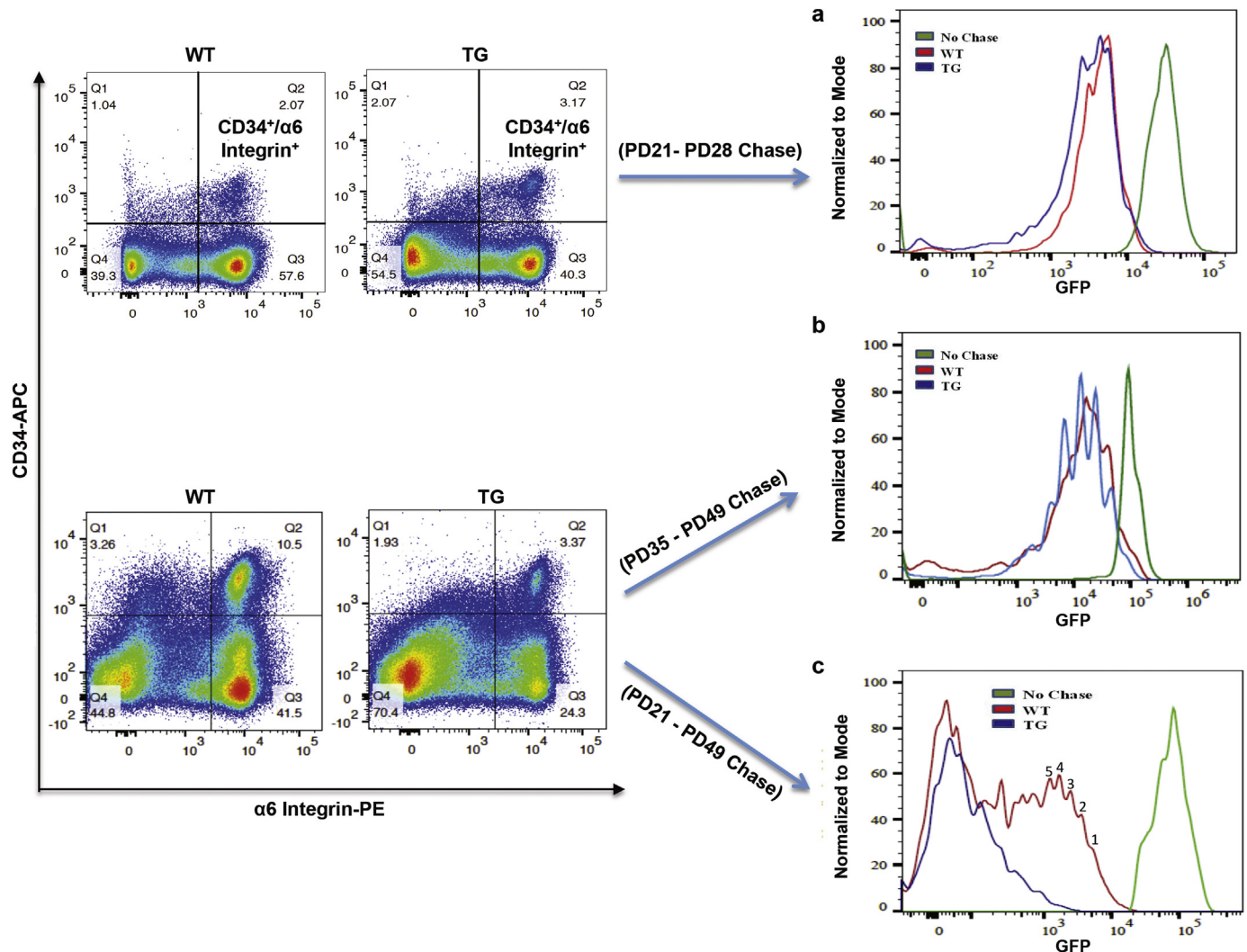
Fig. 2. Altered proliferation dynamics and loss of HFSCs quiescence in K14-sPLA$_2$-IIA mice. a) WT and TG mice were Doxycycline chased (1 g/kg) from PD21 to PD28 and analyzed for H2BGFP dilution in the FACS sorted HFSCs. b) H2BGFP dilution in the FACS sorted HFSCs after Doxycycline chase from PD35 to PD49. c) H2BGFP dilution in the FACS sorted HFSCs after Doxycycline chase from PD21 to PD49. (WT- Wild type for sPLA$_2$-IIA and positive for H2BGFP:K5tTa, TG- K14-sPLA$_2$-IIA:H2BGFP:K5tTa positive mice, $n = 3$ mice/genotype).

mouse model. Five mice per clone/vector control were used for the experiment. Tumour dimensions were measured using a vernier caliper and tumour volume was plotted by using GraphPad prism. The study was approved by the Institutional Animal Ethics Committee (IAEC).

2.10. Real-time PCR (qRT-PCR)

For real-time PCR, total RNA was isolated (Absolutely RNA, Stratagene) from the vector control and sPLA$_2$-IIA shRNA transfected cells. Equal amount (1 μg) of RNA was added to reverse transcriptase reaction mix (Thermo Scientific) and cDNA was synthesized using OligodT primers. Glyceraldehyde phosphate dehydrogenase (GAPDH) was used for normalization. Real-time PCR was performed on QuantStudio 12 K Flex Real-Time PCR System (Thermo Scientific) using SYBR Green master mix. Analysis was carried out using the $2^{-\Delta\Delta Ct}$ method. Primer sequences are included in the Supplementary Table 1.

2.11. Statistical analysis

We used unpaired two-tailed student's *t*-test with GraphPad Prism 5 to calculate the statistical significance for the data of BrdU proliferation assay, depilation study, sphere formation assay, H score calculation, Real Time PCR, and tumour volume. Data is represented with error bar indicating the mean ± SD of the mean: ns- not significant, $^*P < .05$, $^{**}P < .01$, $^{***}P < .001$.

3. Results

3.1. In vivo altered proliferation dynamics of HFSCs in K14-sPLA$_2$-IIA mice

Our previous study showed that the overexpression of sPLA$_2$-IIA in the mice epidermis resulted in depletion of HFSCs (~ 50 to 60%) [21]. These observations led us to further examine if sPLA$_2$-IIA induced proliferation would affect the infrequent SC division kinetics, and whether sPLA$_2$-IIA equally targets all the HFSCs having different quiescent potentials for proliferation? We used the triple transgenic mice (K14-sPLA$_2$-IIA:pTRE-H2BGFP:K5tTa) to understand the proliferation dynamics of HFSCs in the K14-sPLA$_2$-IIA mice (Fig. 1a). We obtained the K14-sPLA$_2$-IIA mice in pTRE–H2BGFP:K5tTa background, however, as the dual combination of the sPLA$_2$-IIA and H2BGFP showed postnatal lethal phenotype, we partially inhibited the H2BGFP expression in the newborn pups by supplying Doxycycline as described in the materials and methods section. We first confirmed the H2BGFP labeling efficiency at first telogen (PD21) (Fig. 1b) in both the WT and K14-sPLA$_2$-IIA mice HFSCs by measuring GFP intensity in FACS sorted CD34 and α6 integrin dual positive cells (Fig. 1c-e), and also by immunofluorescence imaging of GFP (Supplementary Fig. 1a). Our results showed an equal intensity of GFP in the HFSCs of both the WT and K14-sPLA$_2$-IIA mice, which suggests an equal efficiency of the initial labeling. To assess the rate of HFSCs proliferation during anagen phase, we chased mice with Doxycycline (1 g/kg) starting from PD21 to PD28 (telogen to anagen). Our results suggest an additional division of the HFSCs in K14-sPLA$_2$-IIA transgenic
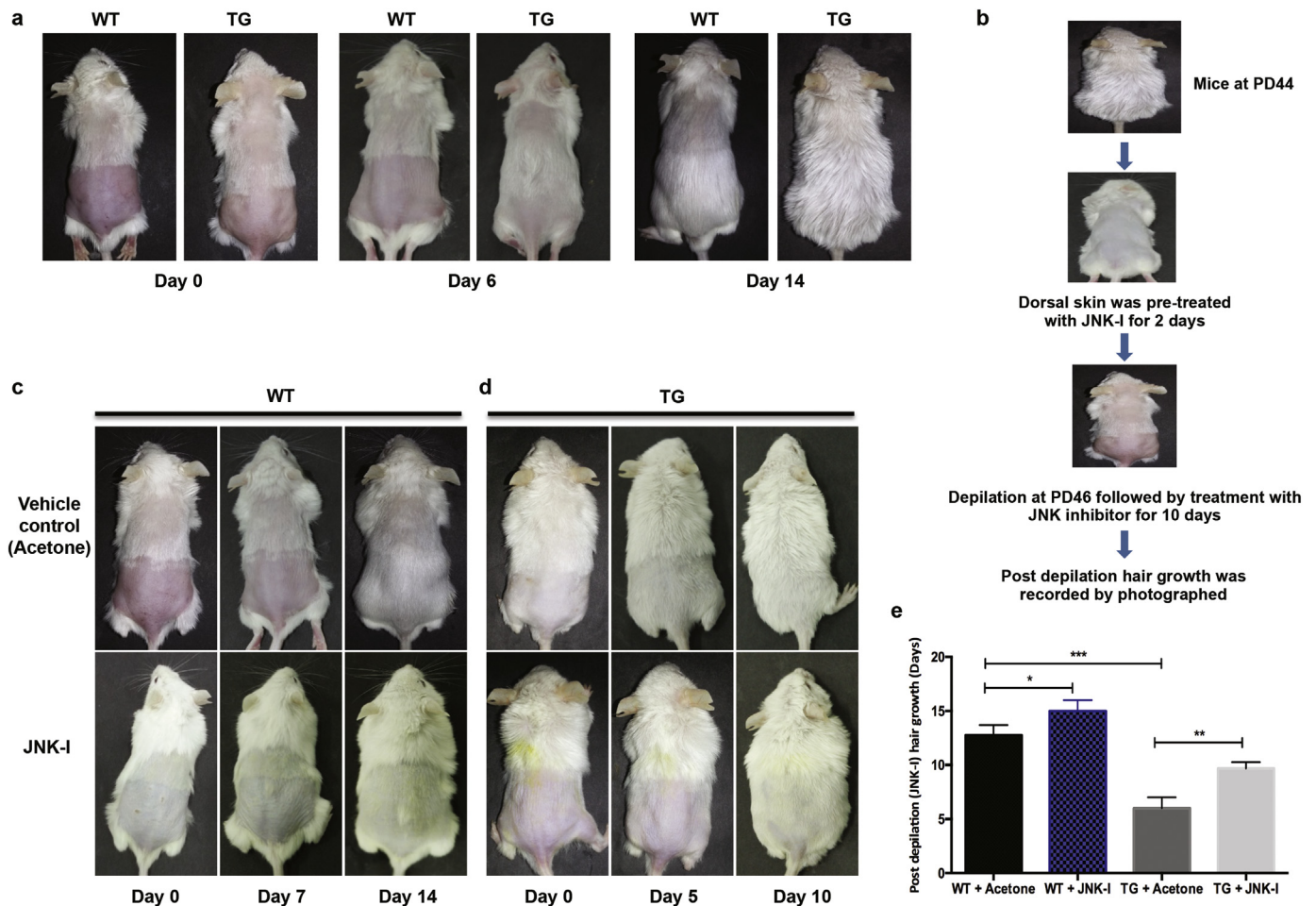
Fig. 3. Functional potentials of HFSCs and *in vivo* reversion of depilation-induced faster hair growth in K14-sPLA$_2$-IIA mice. a) Comparative post depilation hair growth in WT and TG mice at different time points. b) Scheme for the JNK inhibitor (JNK-I) treatment and *in vivo* reversion of the depilation induced faster hair growth analysis. c-d) Comparative post depilation hair growth after topical application of Acetone and JNK-I on WT and TG mice. e) Graphical representation of the number of days required for initiation of post depilation hair growth during different conditions. (WT- Wild type, TG- K14-sPLA$_2$-IIA mice, $n = 5$ mice/genotype, * - $P \le .05$, ** - $P \le .01$, *** - $P \le .001$)

mice (Fig. 2a). Further, we sought to understand if the sPLA₂-IIA induced rapid proliferation was restricted to the anagen phase and whether the activation of repressive signalling after completion of anagen was sufficient to suppress the proliferation of HFSCs. To evaluate this, we chased the mice from PD35 to PD49 (catagen to telogen) (Fig. 1b). Here, we observed multiple divisions of the HFSCs even during both the catagen and telogen phases (Fig. 2b). This suggests that the repressive signalling (such as BMP) during the telogen was not sufficient to inhibit sPLA₂-IIA induced proliferation. To assess the effect of the sPLA₂-IIA induced proliferation on entire hair cycle, the triple transgenic mice were chased starting from PD21 to PD49, which showed loss of bright peaks of H2BGFP positive HFSCs (Peak 1 to 5), indicating loss of slow cycling or quiescent SC population (Fig. 2c and Supplementary Fig. 1b). This was due to the multiple divisions of HFSCs during the entire hair follicle cycle that resulted in the sequential serial dilution of H2BGFP and ultimately led to the exhaustion of H2BGFP positive cells. Together, these data indicate that the sPLA₂-IIA induced rapid proliferation of all the HFSCs, irrespective of their quiescence potential, and altered their infrequent division kinetics *in vivo*.

3.2. Depilation on the dorsal skin induces faster hair growth in K14-sPLA₂-IIA mice.

The loss of quiescence and altered proliferation dynamics of HFSCs led us to investigate whether the remaining (~40 to 50%) and rapidly proliferating HFSCs retain their functional potential or not. Here, we have used depilation approach as the removal of entire hair shaft from the follicle provides mechanical stimulation for the HFSCs activation that further differentiate into hair shaft producing cells. We performed depilation on the lower half of the dorsal skin in both the wild-type and K14-sPLA₂-IIA mice at second telogen (PD46), when HFSCs are known to be in their quiescent state. We recorded comparative hair growth on the upper half (shaved but not depilated) and lower half (shaved and then depilated) of dorsal skin. The result showed that the hair growth was visible in the depilated area of K14-sPLA₂-IIA mice at day 6, but not in wild-type mice as also evident by histological analysis (Fig. 3a and Supplementary Fig. 2a-b). Importantly, we also observed faster hair growth on the upper half dorsal skin of K14-sPLA₂-IIA mice, and complete hair coat recovery was achieved at day 14 (Fig. 3a, e and Supplementary Fig. 3a-b). These data suggest that the remaining HFSCs in K14-sPLA₂-IIA mice were adequate and functionally competent to generate progenitors, which further differentiate to form the entire hair shaft.

3.3. In vivo hair growth reversal by inhibition of JNK/c-Jun signalling

sPLA₂-IIA is known to induce proliferation in multiple cell types. However, the specific downstream targets of sPLA₂-IIA, responsible for the increased proliferation and differentiation remain unknown. In
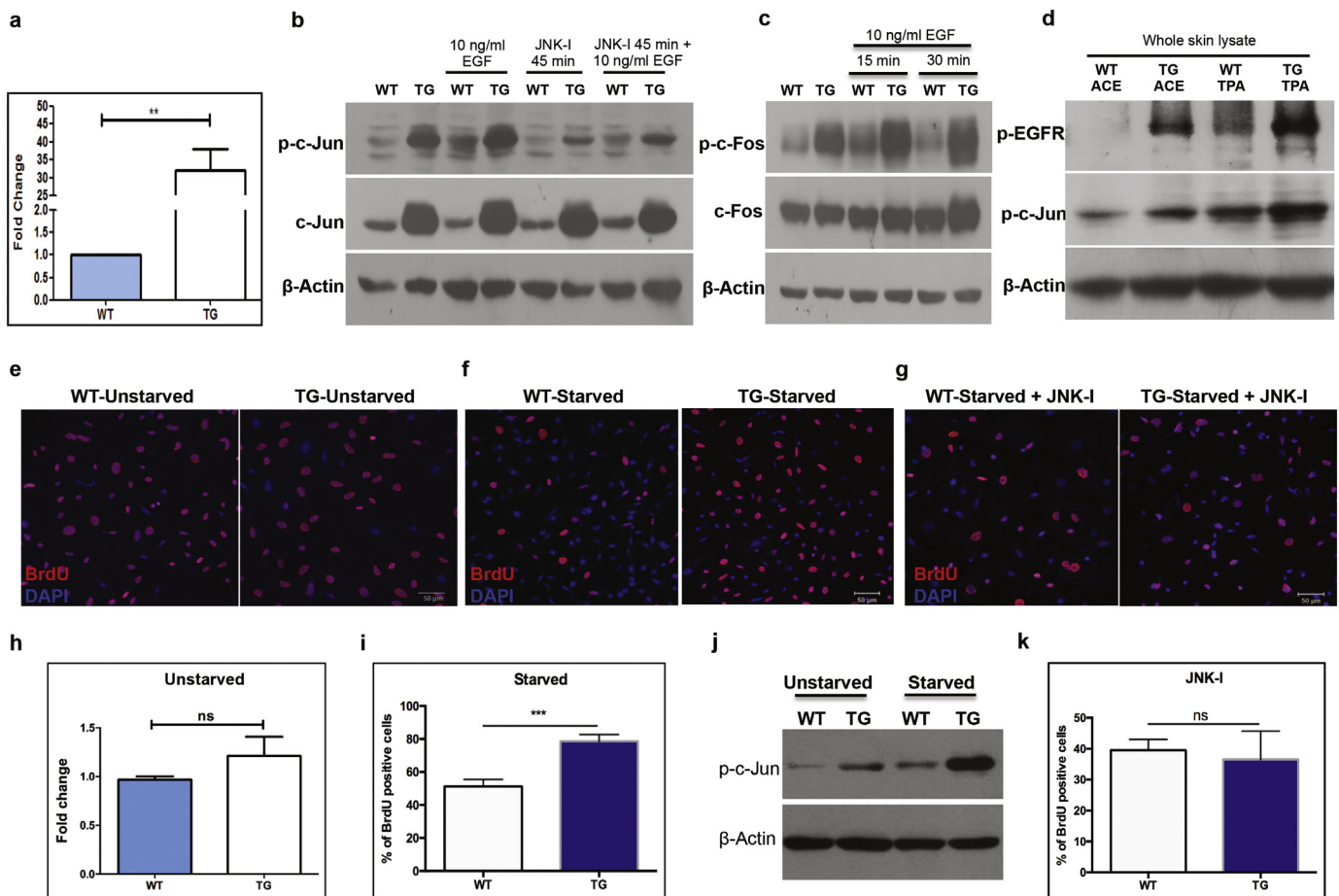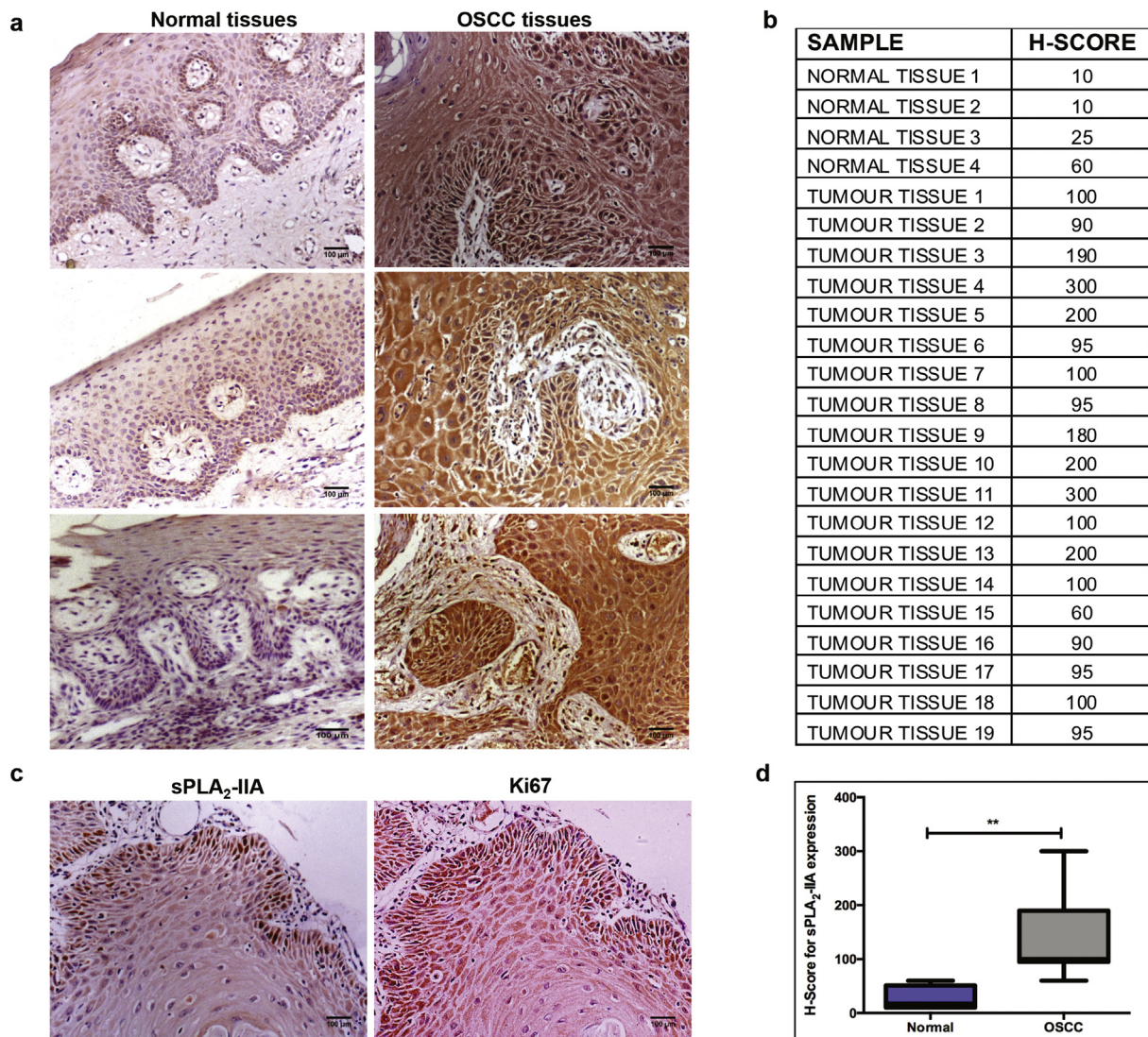

Fig. 4. sPLA₂-IIA induced c-Jun mediates altered AP1 signalling enhances keratinocytes proliferation. a) Real time PCR quantification of PLA2G2A in WT and TG mouse primary keratinocytes *in vitro*. b) Western blot analysis of p-c-Jun and c-Jun after EGF and JNK-I treatment in WT and TG keratinocytes. c) Western blot of p-c-Fos and c-Fos after EGF stimulation in WT and TG keratinocytes. d) Validation of increased activation of EGFR and c-Jun in WT and TG mice epidermis. e) Primary keratinocytes were stimulated with complete *E*-media containing 10 μM BrdU for eight hours and BrdU positive cells were detected by immunofluorescence assay. f) Primary keratinocytes were serum starved for 24 h and stimulated with complete E-media containing 10 μM BrdU for eight hours. g) Primary keratinocytes were starved with JNK-I for 24 h and stimulated with complete E-media containing 10 μM BrdU for eight hours. h-i) Quantification of BrdU⁺ cells in WT and TG mice keratinocytes during unstarved and starved condition. j) Differential activation of c-Jun during unstarved and starved conditions in WT and TG mice keratinocytes. k) Quantification of BrdU⁺ cells after treatment with JNK-I for 24 h in WT and TG mice keratinocytes. (WT- Wild type, TG- K14-sPLA₂-IIA mice, EGF- Epidermal growth factors, JNK-c-Jun N-terminal kinases, ACE- Acetone, TPA- 12-O-Tetradecanoylphorbol-13-acetate, $n = 3$ mice/genotype, ns - $P > .05$, *** - $P \leq .001$)

addition, K14-sPLA$_2$-IIA mice are known to be susceptible to chemical-induced skin carcinogenesis [36]. Therefore, we explored the inhibition study by targeting putative oncogenic signalling mediator c-Jun, which we had observed to be deregulated in HFSCs of K14-sPLA$_2$-IIA mice [21]. To perform the hair growth reversion study, dorsal skin was topically pretreated with JNK-I for two days before depilation, followed by topical application of the JNK-I on the depilated area for 10 days (Fig. 3b). Our results showed minimal effect of JNK-I on the hair growth of wild-type mice (Fig. 3c, e). However, in K14-sPLA$_2$-IIA mice, the hair growth began at day 6 on the depilated dorsal skin of the Acetone treated K14-sPLA$_2$-IIA mice but not on the JNK-I treated dorsal skin of K14-sPLA$_2$-IIA mice, as also shown by histological analysis (Fig. 3d and Supplementary Fig. 2b). Further, long-term topical treatment of JNK-I delayed hair growth till day 10, whereas, Acetone treated K14-sPLA$_2$-IIA mice skin displayed hair growth on the entire depilated area (Fig. 3d, e). In addition, the shaved region followed by the JNK-I treatment has also showed a similar pattern of delay in hair growth as observed in the depilation experiment, albeit the hair growth was slower in the shaved region as compared to depilation (Supplementary Fig. 2a-b and Supplementary Fig. 3a-b). These data suggest that inhibition of JNK mediated signalling was sufficient to suppress sPLA$_2$-IIA induced HFSCs activation and counterbalance depilation induced faster hair growth in K14-sPLA$_2$-IIA mice.

3.4. sPLA$_2$-IIA alters proliferation of mouse epidermal keratinocytes in vitro

We further attempted to explore the detailed mechanism through which sPLA$_2$-IIA induces c-Jun activation *in vitro*. Here, we used primary keratinocytes established from the new-born wild type and K14-sPLA$_2$-IIA mice. The qRT-PCR showed PLA2G2A expression was upregulated in K14-sPLA$_2$-IIA mice keratinocytes as compared to wild type (Fig. 4a). Further, we performed the *in vitro* JNK inhibition study on the mouse primary keratinocytes to explore the possibilities of involvement of other signalling mechanisms for activation of c-Jun. Western blotting analysis showed increased activation of c-Jun and c-Fos in K14-sPLA$_2$-IIA mice epidermal keratinocytes as compared to the wild-type keratinocytes (Fig. 4b-c and Supplementary Fig. 4a-b). Further, to understand the potential involvement of other c-Jun activators in hyperactivation of c-Jun signalling, keratinocytes were treated with JNK-I, which showed that the inhibition of JNK reduces c-Jun phosphorylation after EGF stimulation (Fig. 4b). This data suggest that the EGFR mediated JNK activation was responsible for the enhanced c-Jun activation in K14-sPLA$_2$-IIA keratinocytes. In addition we have performed qRT-PCR on FACS sorted HFSCs, which showed upregulated expression of all the three genes such as c-Jun, c-Fos and AP1 expression in K14-sPLA$_2$-IIA mice HFSCs as compared to WT HFSCs (Supplementary Fig. 5) [21].

SAMPLE	H-SCORE
NORMAL TISSUE 1	10
NORMAL TISSUE 2	10
NORMAL TISSUE 3	25
NORMAL TISSUE 4	60
TUMOUR TISSUE 1	100
TUMOUR TISSUE 2	90
TUMOUR TISSUE 3	190
TUMOUR TISSUE 4	300
TUMOUR TISSUE 5	200
TUMOUR TISSUE 6	95
TUMOUR TISSUE 7	100
TUMOUR TISSUE 8	95
TUMOUR TISSUE 9	180
TUMOUR TISSUE 10	200
TUMOUR TISSUE 11	300
TUMOUR TISSUE 12	100
TUMOUR TISSUE 13	200
TUMOUR TISSUE 14	100
TUMOUR TISSUE 15	60
TUMOUR TISSUE 16	90
TUMOUR TISSUE 17	95
TUMOUR TISSUE 18	100
TUMOUR TISSUE 19	95

Fig. 5. Expression of sPLA$_2$-IIA is upregulated in OSCC tissues. a) IHC staining of sPLA$_2$-IIA in normal cut margin and advanced stage OSCC tumour tissues. b,d) Summary of IHC analysis (H-score) of sPLA$_2$-IIA in normal cut margin and OSCC tumour tissues, and graphical representation of the differential sPLA$_2$-IIA expression. c) IHC staining of sPLA$_2$-IIA and Ki67 on OSCC tumour tissue. (** - $P \leq .01$, Scale bar 100 μm)

This data was further validated in the *in vivo* system by assessing the level of activated EGFR and c-Jun in the whole skin lysate. Our result showed an enhanced activation of EGFR and c-Jun in both the Acetone and TPA treated K14-sPLA$_2$-IIA transgenic mice skin (Fig. 4d and Supplementary Fig. 4c). These data revealed that sPLA$_2$-IIA promotes epidermal proliferation through upregulated c-Jun and c-Fos signalling.

The functional effect of the upregulated EGFR-JNK/c-Jun signalling on the keratinocytes proliferation was assessed by the BrdU incorporation assay. Interestingly, immunofluorescence staining of the BrdU positive cells demonstrated faster proliferation of the K14-sPLA$_2$-IIA mice keratinocytes upon serum starvation-induced synchronization but not in the non-synchronized keratinocytes (Fig. 4e, f, h, i). Therefore, we checked whether c-Jun was differentially activated in the keratinocytes during serum starved and unstarved conditions. Here, the data showed increased activation of c-Jun during serum starvation as compared to the unstarved condition (Fig. 4j and Supplementary Fig. 4d). In addition, we always observed enhanced c-Jun expression in the K14-sPLA$_2$-IIA mice keratinocytes irrespective of the conditions provided. Therefore, we further investigated whether an increased c-Jun activation during the starved condition had any effect on the post-starvation keratinocytes proliferation. The treatment with the JNK-I during the starvation period significantly reduced K14-sPLA$_2$-IIA mice keratinocytes proliferation and it is similar to that of WT keratinocytes during post-starvation stimulation (Fig. 4g, k). Overall, these studies demonstrated that JNK signalling was further enhanced during the serum starvation condition, which provides proliferative advantage to

primary keratinocytes when stimulated with the serum containing media, possibly through c-Jun induced EGFR expression [32].

3.5. sPLA$_2$-IIA is upregulated in epithelial squamous cell carcinoma

To investigate the role of sPLA$_2$-IIA in a different cellular context, and to elucidate whether the sPLA$_2$-IIA induced c-Jun mediated signalling also plays a crucial role in the epithelial tumour cell proliferation, we determined the role of sPLA$_2$-IIA in epithelial-based cancers. We selected both the oral and cutaneous squamous carcinoma cells as both these cell types are derived from the epithelial origin and share many similarities including expression pattern of various keratins. We checked the level of sPLA$_2$-IIA expression in the advanced stage treatment-naive OSCC tissues (19 samples) in comparison with the normal adjacent margin tissues of the Indian oral cancer patients by performing IHC. Our data demonstrated an increased expression of sPLA$_2$-IIA in advanced-stage tumour tissue as compared to the normal adjacent margin tissue (Fig. 5a). The overall staining intensity and number of the positive cells showed increased expression in all tissues analyzed, which is represented in the form of H score (Fig. 5b, d). In addition, our IHC analysis on serial sections of OSCC tumour tissues revealed that sPLA$_2$-IIA and Ki67 express in the same set of cells (Fig. 5c). Apart from the human OSCC tumour tissues, we also analyzed the relative expression and tissue localization of sPLA$_2$-IIA and Ki67 on DMBA/TPA induced mouse skin papilloma and squamous cell carcinoma (SCC) tissues. IHC data showed increased protein levels of sPLA$_2$-IIA in the Ki67 positive
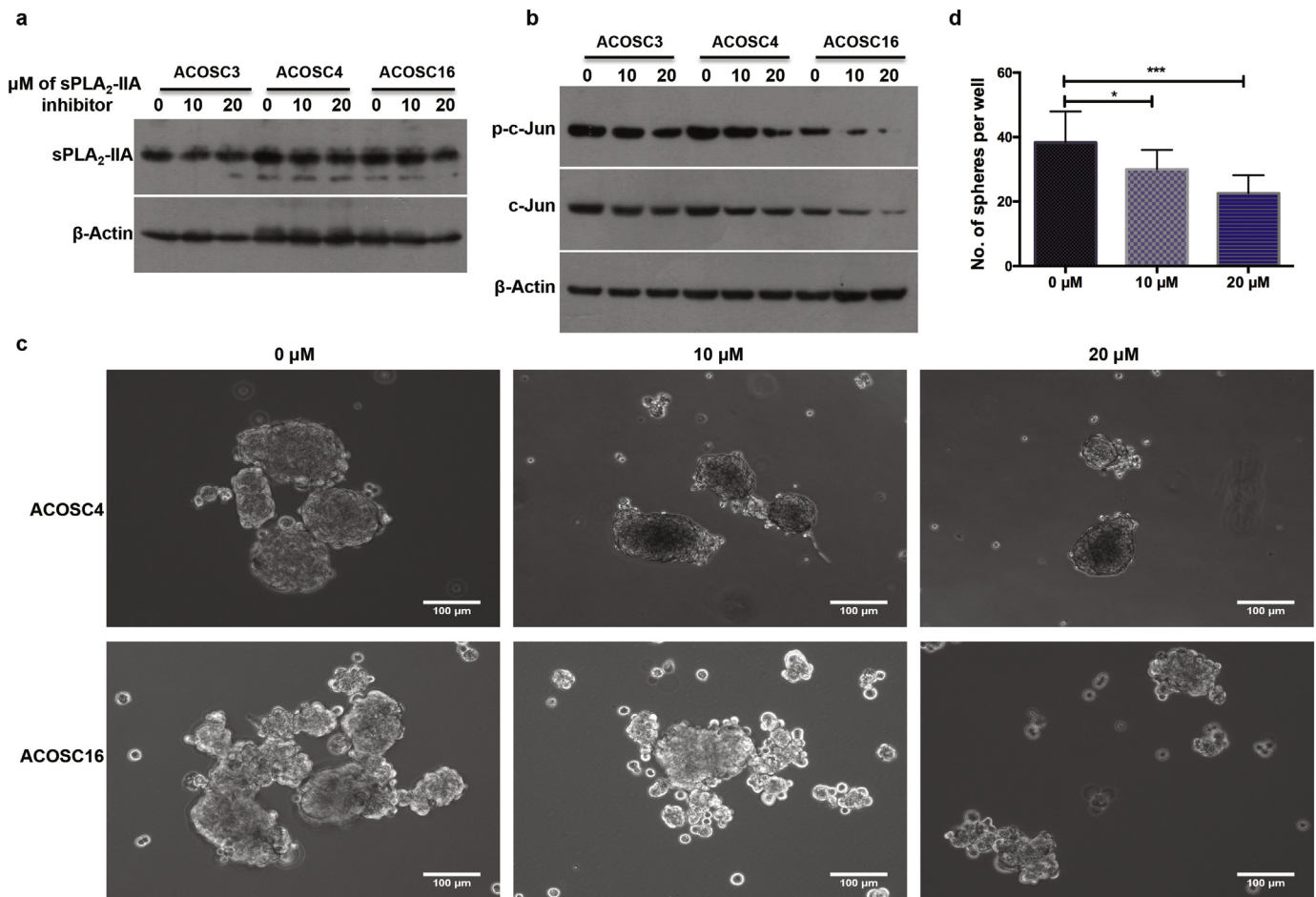
Fig. 6. Inhibition of sPLA$_2$-IIA down regulates JNK/c-Jun signalling and stemness potential *in vitro.* a) Expression of sPLA$_2$-IIA at various time points after sPLA$_2$-IIA inhibitor treatment. b) Effect of sPLA$_2$-IIA inhibitor on the activation and expression of c-Jun in the ACOSC3, ACOSC4, and ACOSC16 cells. c) Sphere formation ability of ACOSC4 and ACOSC16 cells after treatment with different concentrations of sPLA$_2$-IIA inhibitor. d) Quantification of total number of spheres formed per well of the six-well plate. (* - $P \leq .05$, ***- $P \leq .001$, Scale bar 100 μm)

proliferating cells of papilloma as compared to the normal skin, which was enhanced further in SCC tissues (Supplementary Fig. 6a-b). These data suggest that sPLA$_2$-IIA may have proliferation promoting role in the epithelial tumours and may play important role in regulation of tumorigenic potential of the epithelial cells.

3.6. sPLA$_2$-IIA enhances c-Jun signalling in human OSCC cells

To further investigate whether an increased level of sPLA$_2$-IIA in tumour cells had any effect on the downstream signalling cascade, we used sPLA$_2$-IIA specific chemical inhibitor to inhibit the activity of sPLA$_2$-IIA in newly established OSCC cell lines. Cells of the three different cell lines were treated with different concentrations of sPLA$_2$-IIA inhibitor (5 μM, 10 μM and 20 μM) to investigate the effect of sPLA$_2$-IIA inhibition on AP1 signalling. Our western blotting data showed no effect of sPLA$_2$-IIA inhibition on the expression level of the sPLA$_2$-IIA (Fig. 6a). However, a dose-dependent decrease in the level of phosphorylated c-Jun was observed in all the three cell lines (Fig. 6b and Supplementary Fig. 4e). Also, long-term (3 days) treatment of sPLA$_2$-IIA inhibitor demonstrated a decrease in the level of total c-Jun in a dose-dependent

manner (Fig. 6b and Supplementary Fig. 4e). These data demonstrate a direct involvement of sPLA$_2$-IIA in the regulation of c-Jun signalling in OSCC derived tumour cells.

3.7. Inhibition of sPLA$_2$-IIA activity suppresses in vitro tumorigenic potential of OSCC cells

As our study confirmed the involvement of sPLA$_2$-IIA in the activation of c-Jun signalling in both the normal HFSCs and OSCC cells, we sought to understand whether inhibition of sPLA$_2$-IIA activity had any effect on the tumorigenic potential of OSCC cells. Cancer cells have an inherent ability to form spheres when plated on the low adherence surface. We plated 40,000 cells along with different concentrations (0 μM, 10 μM and 20 μM) of sPLA$_2$-IIA inhibitor and counted the number of spheres formed per well. Our results indicated reduced number of spheres in the 10 μM and 20 μM sPLA$_2$-IIA inhibitor treated wells in a dose-dependent manner (Fig. 6c, d). The inhibition of sPLA$_2$-IIA activity resulted in a significant decrease in the ability of OSCC cells to develop spheres, suggesting that the inhibition of the sPLA$_2$-IIA activity reduces the tumorigenic potential of the oral cancer cells.
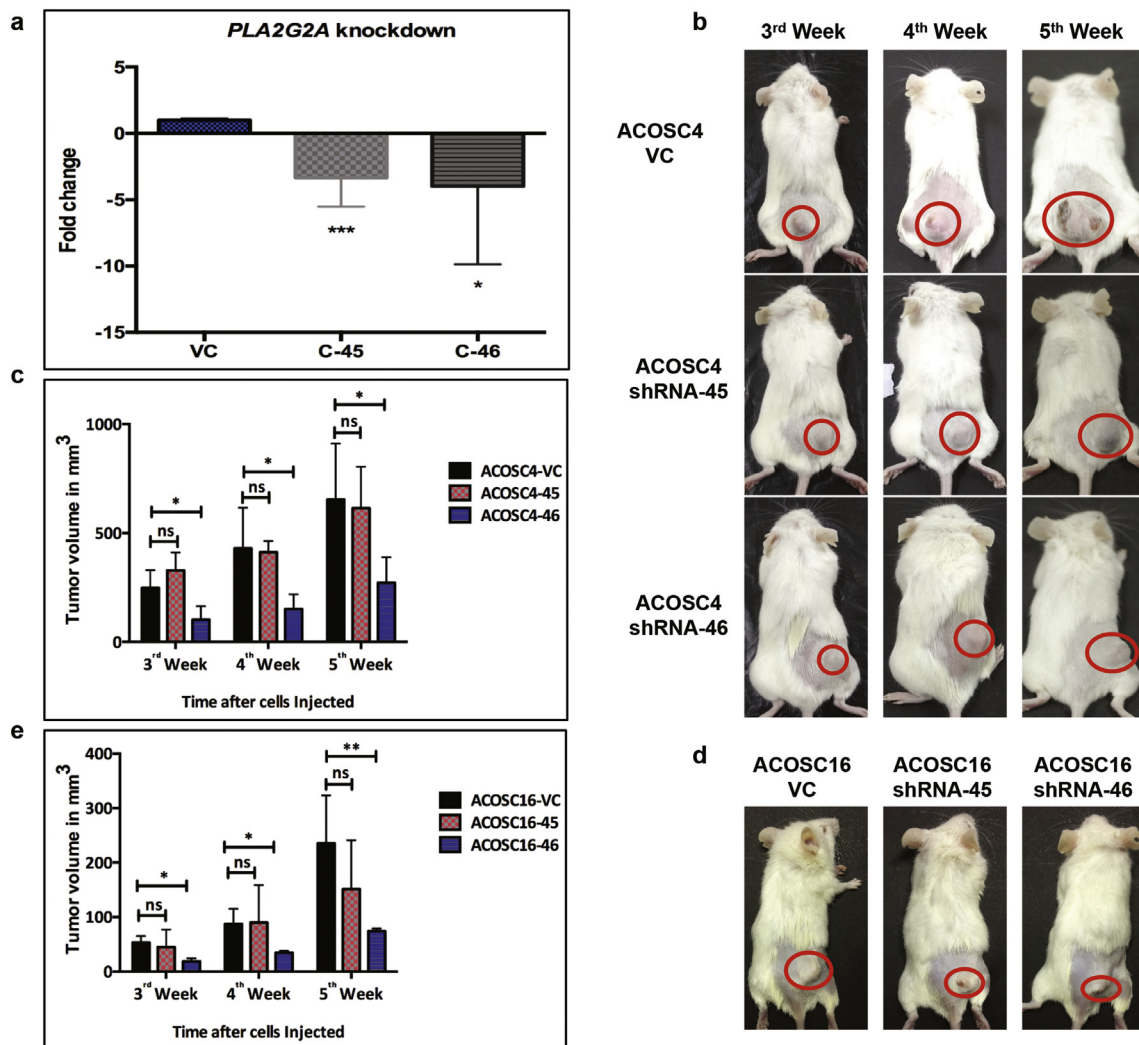
Fig. 7. Knockdown of sPLA$_2$-IIA reduces *in vivo* tumorigenic potential. a) Real-time PCR quantification of *PLA2G2A* in vector control (VC), clone 45 (C-45) and clone 46 (C-46) of the tumour cells. b) Tumour growth in NOD-SCID mice at different time points after injection of VC and *PLA2G2A* shRNA transfected cells of the ACOSC4 cell line. c) Tumour volume in mm^3 at different time points of VC and *PLA2G2A* shRNA transfected ACOSC4 cells. d) Tumour growth in NOD-SCID mice at 5th week after injections of the VC and *PLA2G2A* shRNA transfected cells of the ACOSC16 cell line. e) Tumour volume in mm^3 at different time points of VC and *PLA2G2A* shRNA transfected cells of the ACOSC16 cell line. (VC- Vector Control, ns - $P > .05$, * - $P \leq .05$, **- $P \leq .01$, ***- $P \leq .001$).

3.8. Knockdown of sPLA₂-IIA reduces in vivo tumorigenic potential of oral and skin SCC

Further, to avoid the possibility of the off-target effects of sPLA₂-IIA chemical inhibitor, we performed knockdown of human sPLA₂-IIA in OSCC cell lines by using shRNA technology. The knockdown of sPLA₂-IIA was confirmed by qRT-PCR, which showed significant downregulation of *PLA2G2A* (Fig. 7a). To investigate the role of sPLA₂-IIA in the *in vivo* tumorigenesis, the *PLA2G2A shRNA* transfected cells were injected into NOD-SCID mice, which were then followed for the development of tumours. Our data demonstrated a slower growth of the shRNA transfected cells, specifically the shRNA clone 46 transfected cells *(PLA2G2A shRNA-46)*, in both the ACOSC4 and ACOSC16 cell lines (Fig. 7b, d). This resulted in a smaller size of the tumours and a significant reduction (50 to 60%) in the tumour volume (Fig. 7c, e) as compared to the vector control clones. In addition, we have also checked the role of sPLA₂-IIA in human cutaneous SCC cell line (A3886) by performing knockdown of *PLA2G2A* (Supplementary Fig. 7a). Our results showed a similar decrease in the *in vivo* tumorigenic potential of A3886 cells upon sPLA₂-IIA knockdown (Supplementary Fig. 7b). These data directly highlights the role of sPLA₂-IIA as a proliferation stimulator for the *in vivo* epithelial tumour growth.
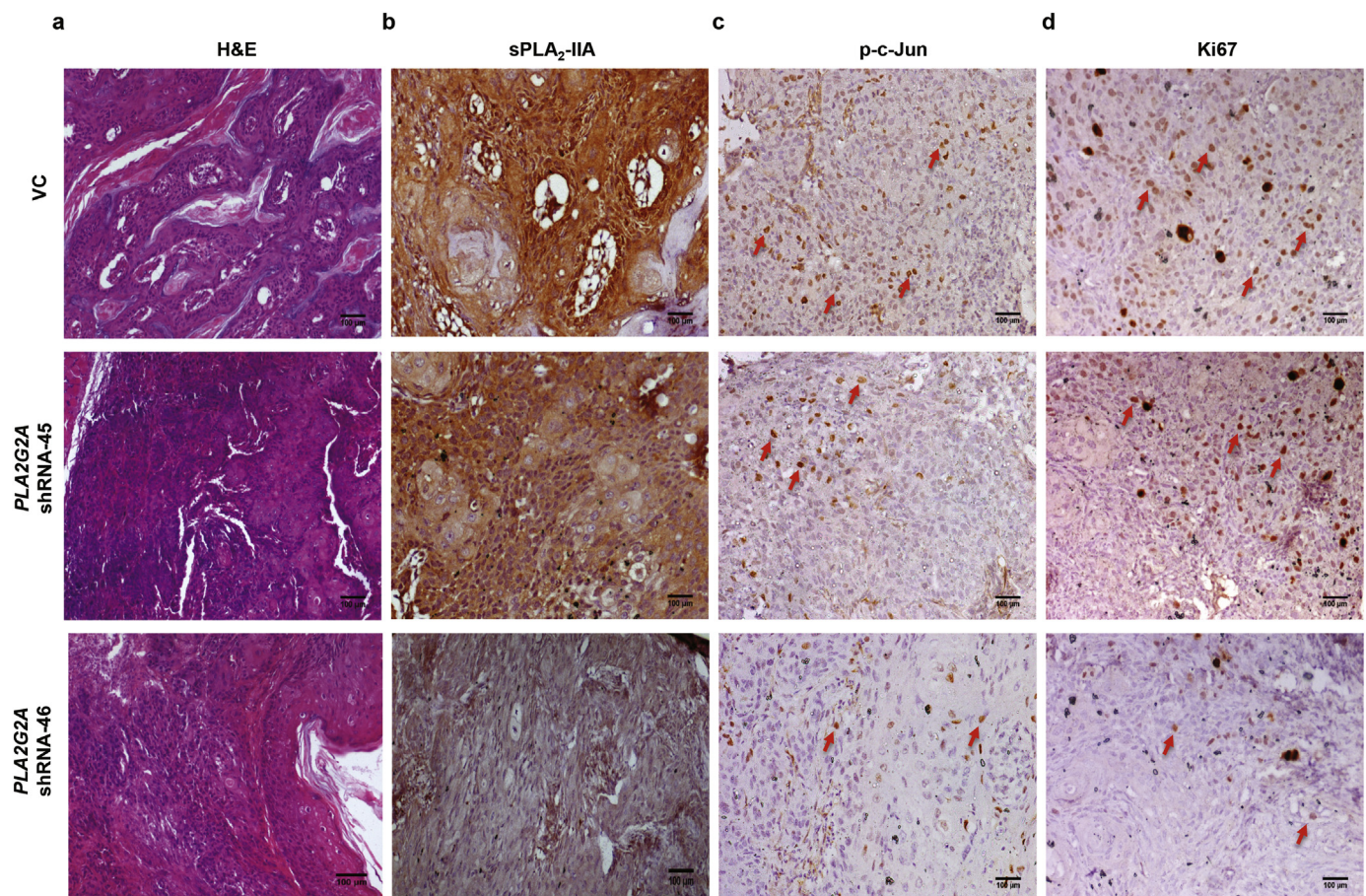
3.9. sPLA₂-IIA knockdown reduces c-Jun signalling and tumour cell proliferation in vivo

We further characterized the tumours developed in the NOD-SCID mice by evaluating the effect of sPLA₂-IIA and c-Jun levels on tumour cell proliferation. We did not observe any difference in the morphological structure of the tumour tissues as assessed by the Hematoxylin and Eosin (H&E) staining (Fig. 8a). Further, the sPLA₂-IIA levels were analyzed in the control tumours as well as in shRNA clone 45 and 46. This data showed reduced level of sPLA₂-IIA in the tumours derived from both the clones; however, the downregulation of the sPLA₂-IIA in tumours of clone 46 was more pronounced as compared to clone 45 (Fig. 8b). Besides, the level of phosphorylated c-Jun was analyzed by IHC staining, which showed decreased activation of c-Jun that correlates with the reduced level of the sPLA₂-IIA (Fig. 8c). Similarly, the lower number of Ki67 positive cells also correlates with the reduced levels of sPLA₂-IIA and c-Jun (Fig. 8d). This data indicated that sPLA₂-IIA activates c-Jun signalling that promotes tumour cell proliferation *in vivo,* and inhibition of sPLA₂-IIA reduces the proliferation and tumorigenic potential of the epithelial cancer cells.

4. Discussion

The family of secretory phospholipase comprises of different isoforms, and their aberrant activities have shown to be involved in various patho-physiological processes. For instance, sPLA₂-IIA is constitutively expressed in inflammatory diseases such as infections, septic shock, and rheumatoid arthritis. In addition, abnormal expression of sPLA₂-IIA has also been reported in diverse human cancers [11–14,41,42]. However, the effect of sPLA₂-IIA induced proliferation on ultimate fate of normal and tumour cells in a different cellular context remains to be investigated. In the present study, we have evaluated the differential effect of sPLA₂-IIA induced proliferation on various cell types of epithelial origin, which have different quiescence and proliferation potential.


Fig. 8. Knockdown of sPLA₂-IIA inhibits c-Jun signalling and cell proliferation in a NOD-SCID tumour. a) H&E staining on the mice tumour tissue derived from the *PLA2G2A* shRNA transfected cells. b) IHC staining of sPLA₂-IIAon the tumours of VC, *PLA2G2A* shRNA-45 and *PLA2G2A* shRNA-46 transfected cells. c-d) IHC staining of p-c-Jun and proliferation marker Ki67 in the tumours of VC, *PLA2G2A* shRNA-45, and *PLA2G2A* shRNA-46 transfected cells. (VC- Vector Control, Scale bar 100 μm)

The HFSCs are highly dynamic and studies have shown heterogeneity in their proliferation rates during the normal hair cycling [2]. In our previous study on K14-sPLA$_2$-IIA mice, we observed 40–50% survival of the HFSCs population (remaining HFSCs population at the end of the first hair cycle at PD49). This data raised two possibilities. First, the sPLA$_2$-IIA induces proliferation of all the HFSCs at a similar rate, irrespective of their quiescence potential and therefore, the remaining population of the HFSCs is a mixture of cells having different quiescence potential. Second, the sPLA$_2$-IIA induced proliferation preferentially targets those SCs, which have low quiescence potential and hence, the remaining HFSCs population contains cells having high quiescence potential. Our results showed that sPLA$_2$-IIA induces proliferation of all HFSCs equally and the remaining HFSCs did not show any bright H2BGFP positive SCs, suggesting that they have divided several times with a loss of GFP intensity. This data explains the mechanism through which persistent mitogenic stimulation leads to the loss of the SC compartment over time as reported by the different studies [43–45]. Moreover, it also suggests that the suppressive signalling for maintenance of the quiescence state after completion of the anagen phase is not sufficient to inhibit the proliferation of the HFSCs during telogen. Importantly, although we observed the proliferation of the HFSCs after completion of the anagen phase in K14-sPLA$_2$-IIA mice, we did not find any significant effect on the maintenance of telogen phase of the hair cycle at PD49 [21]. These data may explain that the remaining partially activated SCs population were not sufficient to independently maintain or induce new anagen phase in K14-sPLA$_2$-IIA mice.

Recent investigation has highlighted the functional involvement of the inner bulge cells in the maintenance of the HFSCs quiescence. The inner bulge cells express Keratin 6, which plays an important role in the inhibition of proliferation of the outer bulge cells during telogen through FGF18 and BMP6 signalling [46]. Interestingly, in this study, we observed the proliferation of HFSCs during telogen. Therefore, we sought to investigate whether the elimination of Keratin 6 positive inner bulge SCs mediated inhibition could induce faster hair growth in the K14-sPLA$_2$-IIA mice, and whether the remaining HFSCs population was sufficient to produce an entirely new hair shaft? The elimination of Keratin 6 positive cells along with hair shaft was achieved by depilation in contrast to shaving, which only removes exterior shafts, leaving the inner root sheath intact. Our results suggest faster hair growth after depilation mediated removal of inner bulge cells in the K14-sPLA$_2$-IIA mice. This data is in agreement with the previous investigations that the entire bulge is not required to induce a new hair follicle regeneration and hair shaft formation [2,38]. Notably, the depilation induced faster hair growth in the K14-sPLA$_2$-IIA mice was mediated through an enhanced JNK/c-Jun signalling. This is in consensus with the study of c-Jun knockout mice, which showed reduced proliferation of basal keratinocytes and smaller papillomas in K5-SOS-F mice mediated due to decreased expression of Hb-EGF and EGFR [31]. Additionally, we have observed that the hair follicle enters into growing phase and hair growth was faster in K14-sPLA$_2$-IIA mice as compared to WT mice even in the shaved region, where the Keratin 6 positive inner bulge and hair shaft are intact. This can be attributed to the accleration in hair cycling with respect to the increased proliferation and differentiation of bulge HFSCs in K14-sPLA$_2$-IIA mice due to enhanced JNK/c-Jun signalling [21]. Collectively, this data explains that balanced c-Jun activity is required to maintain epidermal homeostasis and increased or
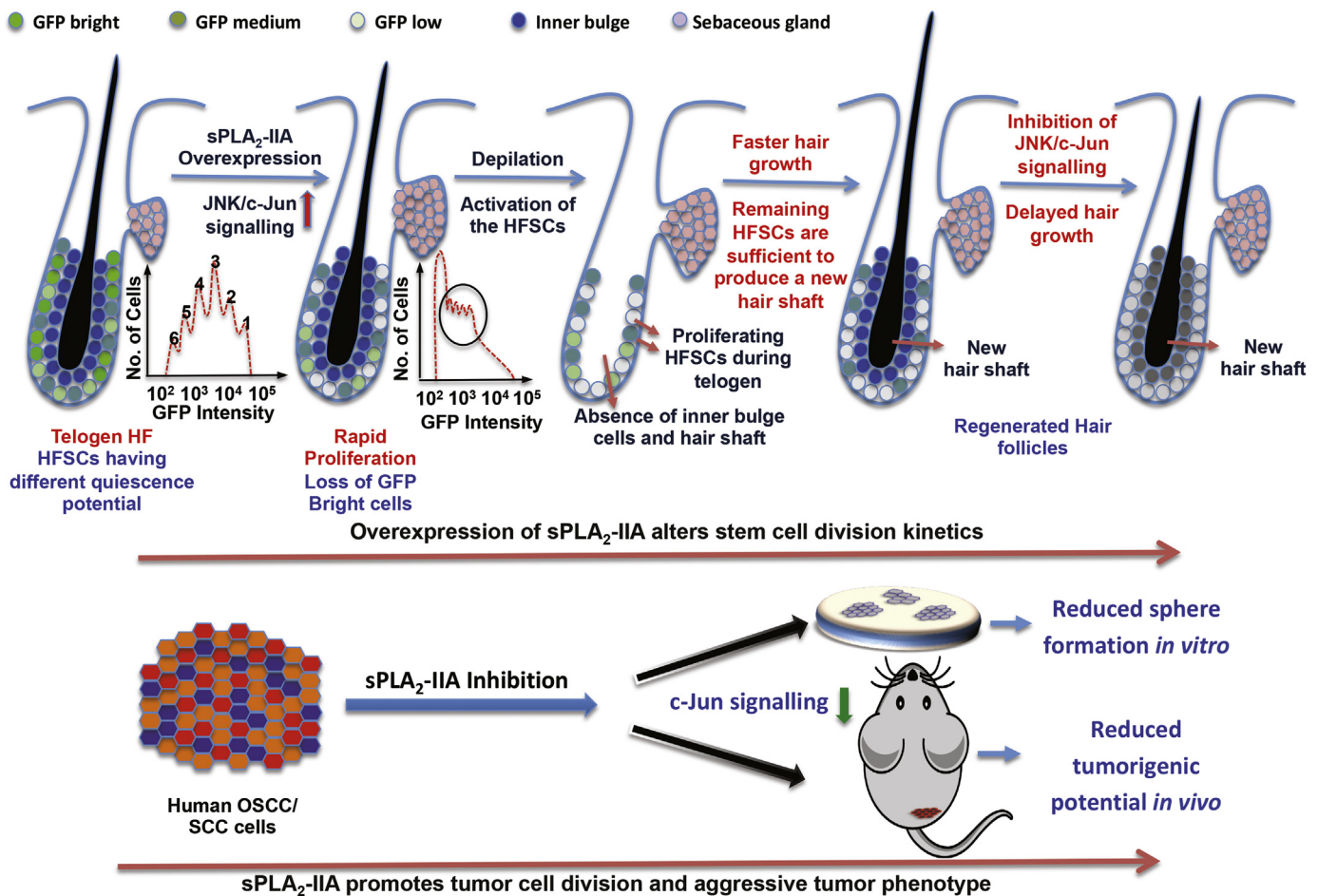
Fig. 9. sPLA$_2$-IIA functions in HFSCs and OSCC/SCC cells. sPLA$_2$-IIA promotes HFSCs proliferation and thereby alters SC division kinetics *in vivo*. The aberrant c-Jun signalling mediated rapid proliferation and hair growth was reverted by inhibition of JNK/c-Jun signalling. In the transformed tumour tissues, sPLA$_2$-IIA increases cell proliferation that leads to an aggressive tumorigenic phenotype and inhibition of the JNK/c-Jun signalling reduces the tumorigenic potential *in vitro* and *in vivo*

decreased level of c-Jun alters proliferation and differentiation of basal keratinocytes [47–49].

sPLA$_2$-IIA has been identified as a tumour susceptible as well as tumour suppressor gene in multiple cancer types. sPLA$_2$-IIA has been shown to be overexpressed in the lung, esophageal adenocarcinoma, and prostate cancers. sPLA$_2$-IIA is also involved in the regulation of cancer stem cells (CSCs) in both the lung and prostate cancer [50,51]. In the present study, chemical and genetic sPLA$_2$-IIA inhibition in human OSCC cells showed reduced ability of sphere formation and decreased *in vivo* tumorigenic potential. Thus, sPLA$_2$-IIA may be involved in the maintenance of oral CSCs, which is similar to lung and prostate CSCs [50,51]. Further, c-Jun is known to regulate EGFR expression in epithelial keratinocytes [31]. Therefore, the observed sPLA$_2$-IIA induced c-Jun activation, in human epithelial cancers such as OSCC and SCC having an aberrant activity of sPLA$_2$-IIA, may explain the fundamental mechanism of the EGFR overexpression mediated pro-proliferative signalling. In addition, a gradual increase observed in the sPLA$_2$-IIA expression, from DMBA/TPA induced papilloma to SCC, strengthen our conclusion that sPLA$_2$-IIA is indeed an important driver for conversion into the malignant tumour phenotype.

Together, we have uncovered a mechanism wherein overexpression of sPLA$_2$-IIA induces proliferation of HFSCs, thereby altering their division kinetics, followed by loss of SC pool. In addition, overexpression of sPLA$_2$-IIA enhances the aggressiveness of cancer cells, which leads to a rapid tumour growth (Fig. 9). Our study provides important insights, as to how deregulated sPLA$_2$-IIA mediated signalling alters cell proliferation, which affects the fate of both the normal SCs and cancer cells in a context-dependent manner.

Acknowledgments

Funding sources

Author contributions

SKW conceived and designed the project, analyzed and interpreted the data; GC, RRS and SRG performed the experiments and analyzed; GC, RRS, SR performed the cell culture, immunostaining and *in vivo* experiments; GC, RRS and SKW analyzed all the data; GC and SKW wrote the manuscript; SKW reviewed the manuscript.

Declaration of Competing Interest

Authors declare no potential conflicts of interest.

Appendix A. Supplementary data

Supplementary data to this article can be found online at https://doi.org/10.1016/j.ebiom.2019.08.053.

References

[1] Tumbar T, Guasch G, Greco V, et al. Defining the epithelial stem cell niche in skin. Science (New York, NY) 2004;303(5656):359–63.

[2] Waghmare SK, Bansal R, Lee J, Zhang YV, McDermitt DJ, Tumbar T. Quantitative proliferation dynamics and random chromosome segregation of hair follicle stem cells. EMBO J 2008;27(9):1309–20.

[3] Waghmare SK, Tumbar T. Adult hair follicle stem cells do not retain the older DNA strands in vivo during normal tissue homeostasis. Chromosome Res 2013;21(3): 203–12.

[4] Li L, Clevers H. Coexistence of quiescent and active adult stem cells in mammals. Science (New York, NY) 2010;327(5965):542–5.

[5] Foudi A, Hochedlinger K, Van Buren D, et al. Analysis of histone 2B-GFP retention reveals slowly cycling hematopoietic stem cells. Nat Biotechnol 2009;27(1):84–90.

[6] Kiel MJ, He S, Ashkenazi R, et al. Haematopoietic stem cells do not asymmetrically segregate chromosomes or retain BrdU. Nature 2007;449(7159):238–42.

[7] Murakami M, Taketomi Y, Sato H, Yamamoto K. Secreted phospholipase A2 revisited. J Biochem 2011;150(3):233–55.

[8] Lambeau G, Gelb MH. Biochemistry and physiology of mammalian secreted phospholipases A2. Annu Rev Biochem 2008;77:495–520.

[9] Chakraborti S. Phospholipase A(2) isoforms: a perspective. Cell Signal 2003;15(7): 637–65.

[10] Quach ND, Arnold RD, Cummings BS. Secretory phospholipase A2 enzymes as pharmacological targets for treatment of disease. Biochem Pharmacol 2014;90(4): 338–48.

[11] Sved P, Scott KF, McLeod D, et al. Oncogenic action of secreted phospholipase A2 in prostate cancer. Cancer Res 2004;64(19):6934–40.

[12] Tribler L, Jensen LT, Jorgensen K, et al. Increased expression and activity of group IIA and X secretory phospholipase A2 in peritumoral versus central colon carcinoma tissue. Anticancer Res 2007;27(5a):3179–85.

[13] Zhang C, Yu H, Xu H, Yang L. Expression of secreted phospholipase A2-group IIA correlates with prognosis of gastric adenocarcinoma. Oncol Lett 2015;10(5):3050–8.

[14] Yu JA, Li H, Meng X, et al. Group IIa secretory phospholipase expression correlates with group IIa secretory phospholipase inhibition-mediated cell death in K-ras mutant lung cancer cells. J Thorac Cardiovasc Surg 2012;144(6):1479–85.

[15] Mauchley D, Meng X, Johnson T, Fullerton DA, Weyant MJ. Modulation of growth in human esophageal adenocarcinoma cells by group IIa secretory phospholipase A(2). J Thorac Cardiovasc Surg 2010;139(3):591–9 [discussion 9].

[16] Hernandez M, Martin R, Garcia-Cubillas MD, Maeso-Hernandez P, Nieto ML. Secreted PLA2 induces proliferation in astrocytoma through the EGF receptor: another inflammation-cancer link. Neuro-oncology 2010;12(10):1014–23.

[17] Martin R, Cordova C, Nieto ML. Secreted phospholipase A2-IIA-induced a phenotype of activated microglia in BV-2 cells requires epidermal growth factor receptor transactivation and proHB-EGF shedding. J Neuroinflammation 2012;9:154.

[18] Gurrieri S, Furstenberger G, Schadow A, et al. Differentiation-dependent regulation of secreted phospholipases A2 in murine epidermis. J Invest Dermatol 2003;121 (1):156–64.

[19] Li-Stiles B, Lo HH, Fischer SM. Identification and characterization of several forms of phospholipase A2 in mouse epidermal keratinocytes. J Lipid Res 1998;39(3): 569–82.

[20] Grass DS, Felkner RH, Chiang MY, et al. Expression of human group II PLA2 in transgenic mice results in epidermal hyperplasia in the absence of inflammatory infiltrate. J Clin Invest 1996;97(10):2233–41.

[21] Sarate RM, Chovatiya GL, Ravi V, Khade B, Gupta S, Waghmare SK. sPLA2-IIA overexpression in mice epidermis depletes hair follicle stem cells and induces differentiation mediated through enhanced JNK/c-Jun activation. Stem Cells 2016;34(9): 2407–17.

[22] Chovatiya GL, Sarate RM, Sunkara RR, Gawas NP, Kala V, Waghmare SK. Secretory phospholipase A2-IIA overexpressing mice exhibit cyclic alopecia mediated through aberrant hair shaft differentiation and impaired wound healing response. Sci Rep 2017;7(1):11619.

[23] Sato H, Taketomi Y, Isogai Y, et al. Group III secreted phospholipase A2 transgenic mice spontaneously develop inflammation. Biochem J 2009;421(1):17–27.

[24] Yamamoto K, Taketomi Y, Isogai Y, et al. Hair follicular expression and function of group X secreted phospholipase A2 in mouse skin. J Biol Chem 2011;286(13): 11616–31.

[25] Yamamoto K, Miki Y, Sato M, et al. The role of group IIF-secreted phospholipase A2 in epidermal homeostasis and hyperplasia. J Exp Med 2015;212(11):1901–19.

[26] Glim JE, van Egmond M, Niessen FB, Everts V, Beelen RH. Detrimental dermal wound healing: what can we learn from the oral mucosa? Wound Repair Regen 2013;21 (5):648–60.

[27] Ta BM, Gallagher GT, Chakravarty R, Rice RH. Keratinocyte transglutaminase in human skin and oral mucosa: cytoplasmic localization and uncoupling of differentiation markers. J Cell Sci 1990;95(Pt 4):631–8.

[28] Presland RB, Dale BA. Epithelial structural proteins of the skin and oral cavity: function in health and disease. Critical Rev Oral Biol Med 2000;11(4):383–408.

[29] Eckert RL, Adhikary G, Young CA, et al. AP1 transcription factors in epidermal differentiation and skin cancer. J Skin Cancer 2013;2013:537028.

[30] Schonthaler HB, Guinea-Viniegra J, Wagner EF. Targeting inflammation by modulating the Jun/AP-1 pathway. Ann Rheum Dis 2011;70(Suppl. 1):i109–12.

[31] Zenz R, Scheuch H, Martin P, et al. C-Jun regulates eyelid closure and skin tumor development through EGFR signaling. Dev Cell 2003;4(6):879–89.

[32] Mishra A, Bharti AC, Saluja D, Das BC. Transactivation and expression patterns of Jun and Fos/AP-1 super-family proteins in human oral cancer. Int J Cancer 2010;126(4): 819–29.

[33] Keren S, Shoude Z, Lu Z, Beibei Y. Role of EGFR as a prognostic factor for survival in head and neck cancer: a meta-analysis. Tumour Biol 2014;35(3):2285–95.

[34] Rubin Grandis J, Melhem MF, Gooding WE, et al. Levels of TGF-alpha and EGFR protein in head and neck squamous cell carcinoma and patient survival. J Natl Cancer Inst 1998;90(11):824–32.

[35] Gkouveris I, Nikitakis NG. Role of JNK signaling in oral cancer: a mini review. Tumour Biol 2017;39(6):1010428317711659.

[36] Mulherkar R, Kirtane BM, Ramchandani A, Mansukhani NP, Kannan S, Naresh KN. Expression of enhancing factor/phospholipase A2 in skin results in abnormal epidermis and increased sensitivity to chemical carcinogenesis. Oncogene 2003;22(13): 1936–44.

[37] Osorio KM, Lee SE, McDermitt DJ, et al. Runx1 modulates developmental, but not injury-driven, hair follicle stem cell activation. Development 2008;135(6):1059–68.

[38] Zhang YV, Cheong J, Ciapurin N, McDermitt DJ, Tumbar T. Distinct self-renewal and differentiation phases in the niche of infrequently dividing hair follicle stem cells. Cell Stem Cell 2009;5(3):267–78.

[39] Gawas NP, Navarange SS, Chovatiya GL, Chaturvedi P, Waghmare SK. Establishment and characterization of novel human oral squamous cell carcinoma cell lines from advancedstage tumors of buccal mucosa. Oncol Rep 2019;41(4):2289–98.

[40] Conway K, Morgan D, Phillips KK, Yuspa SH, Weissman BE. Tumorigenic suppression of a human cutaneous squamous cell carcinoma cell line in the nude mouse skin graft assay. Cancer Res 1992;52(23):6487–95.

[41] Yu JA, Mauchley D, Li H, et al. Knockdown of secretory phospholipase A2 IIa reduces lung cancer growth in vitro and in vivo. J Thorac Cardiovasc Surg 2012;144(5): 1185–91.

[42] Sadaria MR, Yu JA, Meng X, Fullerton DA, Reece TB, Weyant MJ. Secretory phospholipase A2 mediates human esophageal adenocarcinoma cell growth and proliferation via ERK 1/2 pathway. Anticancer Res 2013;33(4):1337–42.

[43] Yamazaki S, Iwamoto R, Saeki K, et al. Mice with defects in HB-EGF ectodomain shedding show severe developmental abnormalities. J Cell Biol 2003;163(3): 469–75.

[44] Yang L, Wang L, Yang X. Disruption of Smad4 in mouse epidermis leads to depletion of follicle stem cells. Mol Biol Cell 2009;20(3):882–90.

[45] Zhou Y, Jiang X, Gu P, Chen W, Zeng X, Gao X. Gsdma3 mutation causes bulge stem cell depletion and alopecia mediated by skin inflammation. Am J Pathol 2012;180 (2):763–74.

[46] Hsu YC, Pasolli HA, Fuchs E. Dynamics between stem cells, niche, and progeny in the hair follicle. Cell 2011;144(1):92–105.

[47] Gazel A, Banno T, Walsh R, Blumenberg M. Inhibition of JNK promotes differentiation of epidermal keratinocytes. J Biol Chem 2006;281(29):20530–41.

[48] Hara T, Miyazaki M, Hakuno F, Takahashi S, Chida K. PKCeta promotes a proliferation to differentiation switch in keratinocytes via upregulation of p27Kip1 mRNA through suppression of JNK/c-Jun signaling under stress conditions. Cell Death Dis 2011;2:e157.

[49] Schumacher M, Schuster C, Rogon ZM, et al. Efficient keratinocyte differentiation strictly depends on JNK-induced soluble factors in fibroblasts. J Invest Dermatol 2014;134(5):1332–41.

[50] Bennett DT, Deng XS, Yu JA, et al. Cancer stem cell phenotype is supported by secretory phospholipase A2 in human lung cancer cells. Ann Thorac Surg 2014;98(2): 439–45 [discussion 45-6].

[51] Lu S, Dong Z. Overexpression of secretory phospholipase A2-IIa supports cancer stem cell phenotype via HER/ERBB-elicited signaling in lung and prostate cancer cells. Int J Oncol 2017;50(6):2113–22.